

LINAC COHERENT LIGHT SOURCE (LCLS) BUNCH-LENGTH MONITOR USING COHERENT RADIATION*

Juhao Wu[†], P. Emma, SLAC, Menlo Park CA 94025, USA

Abstract

The Linac Coherent Light Source (LCLS) is a SASE x-ray Free-Electron Laser (FEL) based on the final kilometer of the Stanford Linear Accelerator. One of the most critical diagnostic devices is the bunch length monitor (BLM), which is to be installed right after each compressor utilizing coherent radiation from the last bending magnet. We describe the components and the optical layout of such a BLM. Based on the setup geometry, we discuss some issues about the coherent radiation signal.

INTRODUCTION

The LINAC Coherent Light Source (LCLS) will be the world's first x-ray Free-electron Laser (FEL) with a Self-Amplified Spontaneous Emission (SASE) operation mode [1]. For a SASE FEL, the bunch length fluctuation ($\Delta\sigma_z/\sigma_z$) will lead to a large fluctuation of the FEL radiation power. For FEL operating in the exponential growth regime, the power fluctuates as $\frac{\Delta P}{P} \approx -\frac{4\pi z \rho}{\sqrt{3}\lambda_w} \frac{\Delta\sigma_z}{\sigma_z}$, where for LCLS parameters, the Pierce parameter $\rho = 5 \times 10^{-4}$, the undulator period $\lambda_w = 3$ cm. At location $z = 100$ m into the undulator, 1 % bunch length fluctuation leads to about 12 % radiation power fluctuation. Hence, the bunch length should be very stable, even though the long undulator length which pushes the FEL well into saturation will reduce the power fluctuation. A longitudinal feedback system is being designed and implemented for LCLS [2]. Within such a longitudinal feedback system, a bunch length monitor (BLM) has to be designed and commissioned for maintaining a stable peak current. A BLM is envisioned as one of the most critical diagnostic devices in the LCLS accelerator system. There are various approaches to diagnose the longitudinal phase space property, and here in this paper, we describe one of the approaches utilizing the coherent radiation from the last bending magnet of the bunch compressor (BC). The concept was introduced in Ref. [3], here in this paper, we will report further development.

SETUP

The first BC is at electron beam energy of $E = 250$ MeV. We will refer it as BC1 in the following. The second one at $E = 4.3$ GeV as BC2. A schematic plot of such a coherent radiation based BLM after BC1 is shown in Fig. 1, and we call it BL11. Coherent Synchrotron Radiation (CSR) is emitted in the last bending magnet when the electron passes through it. In addition, Coherent Edge

Radiation (CER) is produced at the entrance edge and the exit edge of the magnet [4]. Besides CSR and CER, there is also Coherent Diffraction Radiation (CDR) when the electron beam passes through a mirror as shown in Fig. 1.

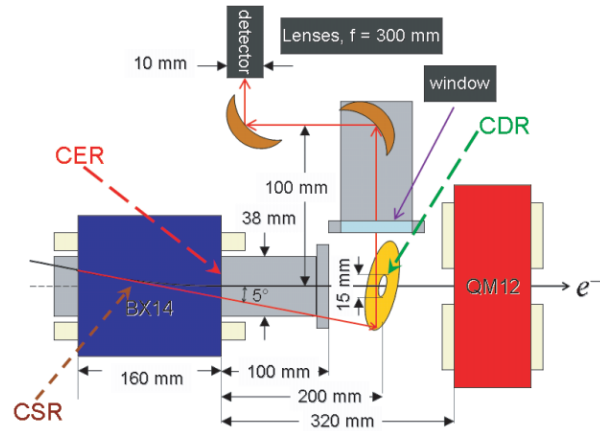


Figure 1: Layout of the LCLS bunch length monitor BL11.

Some details for the BL11 being developed are shown in Fig. 1. The last bending magnet is shown as $BX14$ and the downstream focusing quadrupole is shown as $QM12$. We plan to install a flat mirror at around 200 mm downstream from the edge of the last bending magnet. The mirror is assumed to have an inner diameter of 15 mm and the outer diameter should be large enough to collect all the radiation coupling out of the pipe, which is about 38 mm in diameter and extends for about 100 mm from the edge of the bending magnet. Hence, the mirror will collect both the CSR and the CER from the last bending magnet, and also will generate CDR when the electron beam passes through it. The Coherent Radiation (CR) is directed upwards to the first paraboloid, then reflected on to the second paraboloid, and then reflected into the detectors. We plan to install two pyrodetectors with an optical beam splitter in the optical path. The splitter splits the CR on to the two detectors. The paraboloid has a focal length of $f = 300$ mm. The detailed engineering parameters and design is still evolving. Hence, the calculation and results in this paper should still be regarded as example, and the purpose of this paper is to point out some issues in such a calculation.

SYNCHROTRON RADIATION

There are mainly two issues for our consideration. The first is the near field or far field issue [5]. The observe point is in the far field where the opening angle is independent of the distance, R , between the observation point and the source point. When in the far field regime, the

*Work supported by the U.S. Department of Energy under Contract No. DE-AC02-76SF00515.

[†]jhwu@SLAC.Stanford.EDU

Table 1: Parameters for LCLS BC1 and BC2.

	Q (nC)	ρ (m)	σ_z (μm)	λ (mm)	f (THz)
BC1	1	2.4	200	1.2	0.24
	0.2	2.2	60	0.38	0.8
BC2	1	14	20	0.12	2.4
	0.2	17	8	0.05	6.0

half opening angle $\theta_{\text{open}-1/2}(R, \lambda) = \theta_{\text{open}-1/2}(\infty, \lambda) = (\lambda/\rho)^{1/3}$ with ρ being the bending radius. Hence, the observe point is in the near field, when $R < R_f(\lambda) = \lambda/[\theta_{\text{open}-1/2}(\infty, \lambda)]^2 = \lambda^{1/3}\rho^{2/3}$. For BC1, we have typical $\lambda = 2\pi\sigma_z = 1.2$ mm and $\rho = 2.4$ m, hence, the formation length $R_f \approx 19$ cm. For BC2, $\lambda \approx 0.13$ mm and $\rho = 14.5$ m, hence, the formation length $R_f \approx 30$ cm. The second is the finite length of the bending magnet. For bending magnet with a finite length, the entrance edge and the exit edge have to be taken into consideration. This leads to the edge radiation in our following calculation.

Since in the BC1 current design, the mirror is only 20 cm downstream of the edge of the last bending magnet, the radiation is in the so-called near field regime. It is worthwhile to point out that, for the purpose of introducing the concept, the calculation in Ref. [3] did not consider the real geometry as shown in Fig. 1. The very purpose of this paper is to perform calculation for this particular setup shown in Fig. 1, even though further improvement on the calculation is needed along the development of the BL11.

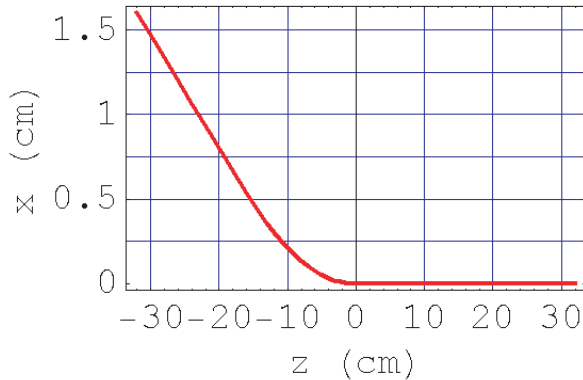


Figure 2: The simplified model of the trajectory.

Single Electron Radiation

The Fourier component of the electric field reads,

$$\mathbf{E}_\omega = \frac{e}{4\pi\epsilon_0 c} \mathbf{F}_\omega, \quad (1)$$

with

$$\mathbf{F}_\omega = i\omega \int_{-\infty}^{\infty} dt' \frac{e^{i\omega t(t')}}{R(t')} \left\{ \vec{\beta}(t') - \left[1 + \frac{ic}{\omega R(t')} \right] \mathbf{n}(t') \right\}. \quad (2)$$

In Eq. (1), e is the charge of the electron, ϵ_0 is the vacuum permittivity; c is the speed of light. In Eq. (2), $\mathbf{R} = \mathbf{r} - \mathbf{r}'$ where $\mathbf{r}(\mathbf{r}')$ is the vector directing from the origin to the observer (electron); $\vec{\beta} = \mathbf{v}/c$ where \mathbf{v} is the velocity of the electron; and $\mathbf{n} = \mathbf{R}/R$ is the unit direction vector. We define the origin of the coordinates on the axis and at the exit-plane of the last bending magnet. Hence, the distance between the electron and the observer, R , is written as $R = [(X-x)^2 + (Y-y)^2 + (Z-z)^2]^{1/2}$ with $\mathbf{r} = (X, Y, Z)$ and $\mathbf{r}' = (x, y, z)$. Following [6], we use electron's longitudinal coordinate z as independent variable, so to write the retarded time t' as

$$t' = \int_0^z \frac{dz'}{c\beta_z} = \frac{1}{c} \int_0^z \left[1 + \frac{1}{2\gamma^2} + \frac{\beta_x^2}{2} + \frac{\beta_y^2}{2} \right] dz'. \quad (3)$$

Notice that we set the integral lower limit as $z' = 0$ for convenience. The retard condition determines the time $t = t' + R(t')/c$ in Eq. (2) as

$$t = \frac{1}{c} \left[z + \frac{z}{2\gamma^2} + \frac{1}{2} \int_0^z (\beta_x^2 + \beta_y^2) dz' + \sqrt{(X-x)^2 + (Y-y)^2 + (Z-z)^2} \right]. \quad (4)$$

Notice also that, according to Eq. (3), we have the Jacobian dt'/dz . The spectral flux density is calculated as

$$\frac{d^2 N_p}{dS d\omega/\omega} = \frac{d^2 \mathcal{E}}{\hbar dS d\omega} = \frac{\epsilon_0 c}{\hbar \pi} |\mathbf{E}_\omega|^2 = \frac{\alpha}{4\pi^2} |\mathbf{F}_\omega|^2, \quad (5)$$

where $\alpha = e^2/(\hbar c 4\pi\epsilon_0) \approx 1/137$ is the fine structure constant with $\hbar = h/(2\pi)$ and $h \approx 6.626 \times 10^{-34}$ is the Planck's constant.

Trajectory

For the setup in Fig. 1, the trajectory is simply modelled as what is in Fig. 2 and expression is given in Table 2. Notice that, $y = 0$ and $\beta_y = 0$ for the reference particle.

Table 2: Trajectory and velocity.

	$z < -z_{\text{dip}}$	$-z_{\text{dip}} < z < 0$	$z > 0$
$x(z)$	$\rho - \frac{zz_{\text{dip}} + \rho^2}{\sqrt{\rho^2 - z_{\text{dip}}^2}}$	$\rho - \sqrt{\rho^2 - z^2}$	0
$\beta_x(z)$	$-\frac{z_{\text{dip}}\beta}{\rho}$	$\frac{z\beta}{\rho}$	0
$\beta_z(z)$	$\frac{\beta}{\rho} \sqrt{\rho^2 - z_{\text{dip}}^2}$	$\frac{\beta}{\rho} \sqrt{\rho^2 - z^2}$	β

EXAMPLES

We work out an example for BL11 to illustrate some issues. We compute the spectral flux density for $\omega = c/\sigma_z$ in the $Y = 0$ plane.

Near Field Edge Radiation

When $R \ll \lambda\gamma^2$, with a “zero edge length” model, the edge radiation field is approximately equal to [4]

$$E(R, \theta) = \frac{e\gamma^2\theta}{\pi\epsilon_0 cR} \left[-i \exp\left(\frac{-i\pi R\theta^2}{2\lambda}\right) \right] \times \frac{\sin[\pi R\theta^2/(2\lambda)]}{1 + \gamma^2\theta^2}. \quad (6)$$

For a finite length magnet, the entrance edge and the exit edge both generate edge radiation, even though the generated field are directing in opposite direction.

Far Field Storage-Ring Synchrotron Radiation

The synchrotron radiation from a storage-ring in the far field regime reads [7]

$$E(R, \theta) = -\frac{\sqrt{3}e\gamma}{4\pi\epsilon_0 cR} \left(\frac{\omega}{\omega_c}\right) (1 + \gamma^2\theta^2) \times \left[\text{sign}(1/\rho) K_{2/3}(\xi) \mathbf{u}_\sigma - i \frac{\gamma\theta K_{1/3}(\xi)}{\sqrt{1 + \gamma^2\theta^2}} \mathbf{u}_\pi \right], \quad (7)$$

where $\omega_c = 3c\gamma^3/(2\rho)$; $r_e = e^2/(4\pi\epsilon_0 mc^2) \approx 2.82 \times 10^{-15}$ m is the classical radius of electron; and $\xi = \frac{1}{2} \frac{\omega}{\omega_c} (1 + \gamma^2\theta^2)^{3/2}$.

RESULTS AND DISCUSSION

In Fig. 3, the dots are for the numerical result for finite bending magnet; the solid curve is for the near field edge radiation including both entrance edge and the exit edge; and the dashed curve is for the storage-ring result. The conventional synchrotron far field result extends to about $X = -2$ cm, and peaks around $X = -1$ cm. It contains both the σ -mode and the π -mode contribution. The edge radiation shows the interference pattern originated from the entrance edge and the exit edge. The numerical result nicely show the contributions from the entrance edge, the body of the bending magnet, and the exit edge. Since the mirror has a hole with a diameter of 1.5 cm, part of the synchrotron radiation from the body part of the magnet leaks out.

Having the comparison in Fig. 3, we understand the contribution of what is normally called edge radiation and what is synchrotron radiation. We can then compute the coherent radiation. Assuming a detector responding to a central wavelength of $\lambda = 2.2$ mm, and a response bandwidth of $\Delta\lambda = 1$ mm, the coherent radiation within in this frequency region at the mirror is shown in Fig. 4. The dashed curve is obtained based on Eq. (6) and stands for the contribution from the edge radiation. The long-dashed curve is from Eq. (7) and stands for the storage-ring synchrotron radiation. The solid curve is the sum of them. As we expected, the edge radiation contribution dominates. The CDR from the mirror is negligible because it is small in the absolute value, and also it is not in the focal plane.

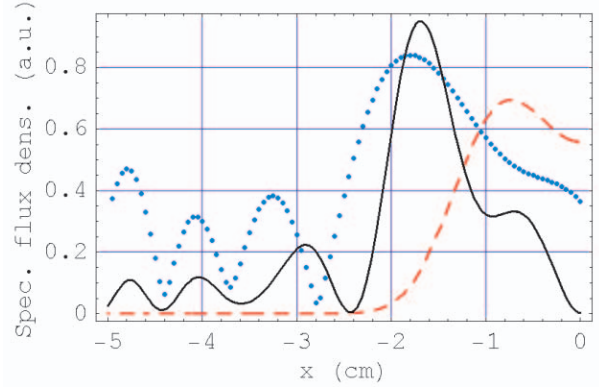


Figure 3: Comparison of the three contributions. Notations are explained in the text.

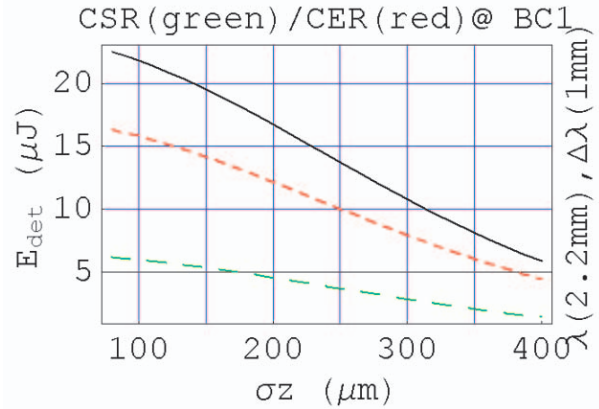


Figure 4: Comparison of CSR and CER. Notations are explained in the text.

Because of the fact that the mirror is close to the bending magnet and the bending magnet has a finite length, some details for calculating the coherent radiation signal is discussed in this paper. Further improvement of the calculation is always possible and needed with the development of the BLMs for LCLS.

REFERENCES

- [1] J. Arthur *et al.*, SLAC-R-593, 2002.
- [2] J. Wu, P. Emma, and L. Hendrickson, PAC-05, p. 1156, Knoxville, TN, 2005.
- [3] J. Wu, P. Emma, and Z. Huang, PAC-05, p. 428, Knoxville, TN, 2005.
- [4] R.A. Bosch and O.V. Chubar, AIP Conf. Proc. **417**, p. 35 (1997).
- [5] D.J. Winham, Phys. Rev. D **35**, 2584 (1987).
- [6] T. Tanaka and H. Kitamura, *J. Synchrotron Rad.*, **8**, 1221 (2001).
- [7] H. Wiedemann, *Synchrotron Radiation*, (Springer-Verlag Berlin Heidelberg, 2003).